Joint Image Registration and Fusion for Panchromatic and Multispectral Images

Qian Zhang, Zhiguo Cao, Zhongwen Hu, Yonghong Jia, and Xiaoliang Wu

***Abstract*—Both image registration and fusion are essential steps to produce high-resolution multispectral images in remote sensing. Traditionally, they are viewed as two independent processes. As a result, the registration errors ignored in the fusion process can significantly affect the fusion quality. In this context, an iterative optimization approach, which jointly considers the registration and fusion processes, is proposed for panchromatic (PAN) and multispectral (MS) images. Given a registration method and a fusion method, the joint optimization process is described as finding the optimal registration parameters to gain the optimal fusion performance. In our approach, the downhill simplex algorithm is adopted to refine the registration parameters iteratively. Experiments on a set of PAN and MS images of ZY-3 and GeoEye-1 show that the proposed approach outperforms several competing ones in terms of registration accuracy and fusion quality.**

***Index Terms*—Image fusion, image fusion quality, image registration, iterative optimization, registration accuracy.**

I. Introduction

IMAGE registration is a crucial step in many remote sensing applications, such as image fusion, change detection, image mosaicing, and map updating [1]. In general, registration methods can be divided into two categories: area-based and feature-based methods. In area-based methods, the image intensity of corresponding regions is used for matching, while in feature-based methods, features on points, lines, and regions are used. In remote sensing, area-based methods are sensitive to the intensity changes and local distortions of satellite images. Due to the limitation of area-based methods, feature-based methods are commonly used for remote sensing image registration [2]. Recently, scale-invariant feature transform (SIFT) [3] is widely and successfully applied in remote sensing image registration, owing to its good characteristics of being invariant to image scaling, rotation, change in illumination, and sensor viewpoint [4].

Image fusion is a technique used to integrate the geometric detail of a high-resolution panchromatic (PAN) image and the color information of a low spatial resolution multispectral (MS) image to produce a high-resolution MS image [5]. There are two limitations of current fusion techniques: the distortion in color and the performance instability to varied data sets. To reduce the color distortion and improve the fusion quality, a wide variety of fusion methods have been presented up to now. According to Aiazzi's advices [6], these methods can be roughly categorized into the component substitution (CS) methods and the multiresolution analysis methods by their protocol. Synthetic variable ratio (SVR) [7], as the representative fusion method of the CS technique, has been a popular method due to its clear physical meaning and theoretical basis, particularly when it was commercialized in PCI Geomatica software [8].

Although various algorithms have been proposed for image registration and image fusion, they are traditionally viewed as two independent processes. In addition, the quality of image registration and that of image fusion are also evaluated separately. The registration accuracy is often evaluated using the root mean square error (RMSE), while the fusion quality is usually assessed using image quality indexes between the original and the fused MS images, such as the correlation coefficient (CC), relative global dimensional synthesis error (ERGAS) [9], and Q4 [10]. Due to the separation of the registration process and the fusion process, the fusion quality will be highly dependent on the registration results, and the registration errors ignored in the fusion process can significantly affect the fusion quality [11], [12].

Chen *et al.* [13] presented a maximum likelihood approach to joint image registration and fusion. The approach is predicated on the assumption that the registration error should be limited within a certain range. Meanwhile, the specific fusion process of the approach is predicated on the assumption that images hold the same value within a certain window [13]. In this letter, a novel optimization approach, which considers jointly the registration and fusion processes, is proposed for PAN and MS images. The advantages of the proposed approach are its robustness and simplicity. In our approach, the downhill simplex algorithm is employed to solve the joint optimization process, where the fusion quality is used as a measure to refine the registration. It avoids the limit of the obvious geometric difference owing to its existing initial registration process, and it can employ a different registration and fusion method in the joint optimization framework.

The contributions of this work lie in two aspects: 1) The fusion quality is used to evaluate the registration accuracy, and 2) a novel joint image registration and fusion approach is

Manuscript received March 19, 2014; revised June 5, 2014 and July 6, 2014; accepted July 29, 2014. This work was supported in part by the National Natural Science Foundation of China under Grant 41001260 and in part by the Fundamental Research Funds for the Central Universities under Grant 201121302020003.

Q. Zhang and Z. Cao are with the National Key Laboratory of Science and Technology on Multi-spectral Information Processing, School of Automation, Huazhong University of Science and Technology, Wuhan 430074, China (e-mail: hangfanzq@163.com; zgcao@hust.edu.cn).

Z. Hu is with the Shenzhen Key Laboratory of Spatial Smart Sensing and Services, Mapping and GeoInformation, College of Civil Engineering, Shenzhen University, Shenzhen 518060, China (e-mail: zhongwenhu@163.com).

Y. Jia is with the School of Remote Sensing and Information Engineering, Wuhan University, Wuhan 430079, China (e-mail: yhjia2000@sina.com).

X. Wu is with the Division of Mathematics, Informatics and Statistics, Commonwealth Scientific and Industrial Research Organization, North Ryde, N.S.W. 2113, Australia (e-mail: xiaoliang.wu@csiro.au).

Color versions of one or more of the figures in this paper are available online at http://ieeexplore.ieee.org.

Digital Object Identifier 10.1109/LGRS.2014.2346398

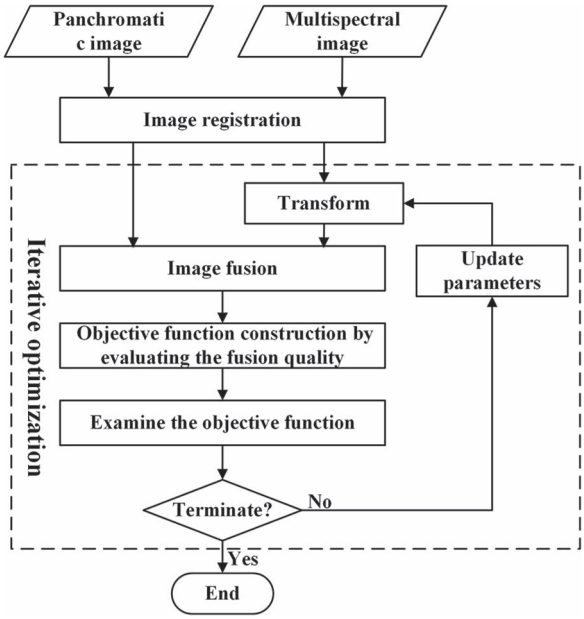

Fig. 1. Workflow of the proposed approach.

proposed, in which the downhill simplex algorithm is adopted to refine the registration parameters. The rest of this letter is organized as follows. The proposed approach is described in Section II, the experimental results and discussions are presented in Section III, and the conclusions are given in the last section.

II. Iterative Optimization Approach

Fig. 1 shows the main steps of the proposed approach. Given a registration method and a fusion method, the joint optimization process is described as finding the optimal registration parameters to gain the optimal fusion performance. To achieve this goal, an iterative strategy is adopted. First, the registered result of the MS image is obtained according to the initial transformation parameters, which are estimated via image registration. Next, the fused image is produced, and the fusion quality is assessed for objective function construction. Finally, the registration parameters are updated iteratively by examining the objective function.

A. Transformation Parameter Estimation

Given a reference image and a sensed image, the registration process aims to find an optimal transformation between the two images. In this letter, let us consider the PAN image as the reference image and the MS image as the sensed image. The transformation from MS image to PAN image can be represented as

$$\begin{cases} x = p_1 + p_2 u + p_3 v \\ y = p_4 + p_5 u + p_6 v \end{cases} \tag{1}$$

where (x, y) and (u, v) denote the pixel coordinates of the PAN and MS images, respectively, and the affine transformation parameters $P = (p1, p2, p3, p4, p5, p6)$.

Once the matched features are detected from PAN and MS images, the transformation parameters are estimated by least squares solution using the affine transformation model.

B. Objective Function Construction

In our approach, the fusion quality is used to evaluate the registration accuracy. When the reference image and the sensed image are precisely matched, the fusion quality should be optimal. As the registration error increases, the fusion quality begins to decrease. Therefore, we construct an objective function F to evaluate the registration accuracy using fusion quality.

Inspired by Kim *et al.* [14], the joint optimization process of image registration and fusion process can be described as finding the transformation parameters P that minimize the objective function F. It can be defined as

$$\hat{P} = \arg\min_{P} F(A, B; P) \tag{2}$$

where P represents the transformation parameters and A and B denote the PAN and MS images, respectively.

The ERGAS index, which is considered as F, is chosen to evaluate the quality of the fused image, considering its running efficiency and its high sensitivity to registration errors. The ERGAS index is represented as [9]

$$\text{ERGAS} = 100\frac{\text{h}}{l}\sqrt{\frac{1}{N_b}\sum_{i=1}^{N_b}\left(\frac{\text{RMSE}_\text{F}^2(B_i)}{M_i^2}\right)} \tag{3}$$

where h is the resolution of the high-resolution PAN image, l is the resolution of the low spatial resolution MS image, N_b is the number of MS bands involved in the fusion, M_i denotes the mean gray value of the ith band of the registered MS image, which is resampled to the size of the PAN image, and $\text{RMSE}_\text{F}(B_i)$, computed in the following expression, represents the difference in spectral information between the ith band of the fused MS image and that of the registered MS image:

$$\text{RMSE}_\text{F}(B_i) = \sqrt{\frac{1}{WH}\sum_{x=1}^{W}\sum_{y=1}^{H}\left[MS_i(x,y) - Fused_i(x,y)\right]^2} \tag{4}$$

where W and H denote the width and the height of the fused image and $MS_i(x, y)$ and $Fused_i(x, y)$ represent the gray value of the ith band of the registered MS image and the fused image at the coordinate of (x, y), respectively.

The lower the value of the ERGAS index, the better the global spectral quality of the fused images. When the ERGAS index obtains the minimum value, the corresponding transformation parameters are the solution of the joint optimization process.

C. Iterative Optimization

In order to minimize the objective function, the downhill simplex method [15] is adopted in this letter. It is a technique for minimizing an objective function in a multidimensional space. It is started with N+1 points by defining an initial simplex, which consists of an initial estimate of the parameter vector and N other vectors [15].

In our approach, we first construct the initial simplex by separating the initial parameter vector along six parameter axes based on affine transformation [16]

$$P_i = P_0 + \lambda n_i, \quad i = 1, 2, \ldots, 6 \tag{5}$$

where P_0 represents the initial affine transformation parameters, λ denotes a constant for the initial simplex, and n_i's are

six vectors. Each parameter value of n_i has a different property and scale due to the affine transformation model.

Then, the objective function value is calculated for every point in a simplex. According to the function values, the method iteratively determines a new simplex based on the movement, reflection, expansion, and contraction steps, whose detailed explanation can be found in [15].

The maximum number of iterations N_{it} is set in the iterative optimization process. In addition, we set the terminating condition of the optimization procedure as

$$\frac{|F_{\max} - F_{\min}|}{|F_{\max}| + |F_{\min}|} < \varepsilon \tag{6}$$

where $F_{\max}$ and $F_{\min}$ denote the maximum and the minimum objective function value of points in the simplex, respectively, and ε is the precision tolerance.

The detailed steps of the iterative optimization process are listed as follows:

Algorithm 1 The Iterative Optimization Algorithm

Input: initial affine transformation parameters P_0.
Output: refined transformation parameters $\hat{P}$.
1: Let $n=0$, and set the stop condition (including maximum iteration number N_{it} and precision tolerance ε).
2: Construct the simplex $P_i = P_0 + \lambda n_i, i = 1, 2, \ldots, 6$.
3: **while** $n \leq N_{it}$ **do**
4: **for** each $i \in [0, 6]$ **do**
5: Transform the sensed image using P_i. Produce the fused image.
6: Calculate the objective function F_i by ERGAS index.
7: **end for**
8: Determine $F_{\max}$ and $F_{\min}$. Find the index $i_{\min}$ of $F_{\min}$.
9: **if** $(|F_{\max} - F_{\min}|/|F_{\max}| + |F_{\min}|) < \varepsilon$ **do**
10: Set $\hat{P}$=$P_{i_{\min}}$. Break
11: **end if**
12: Determine the new simplex P_i via movement, reflection, expansion, and contraction steps.
13: $n = n + 1$.
14: **end while**

III. Experiments and Discussions

In this section, experiments and comparisons were carried out to validate the effectiveness of the proposed approach, which is implemented in C++. In the following, first, the testing data sets are introduced, and then, experiments and discussions are provided.

A. Experimental Data Sets

In our experiments, two data sets are used to evaluate the performance of the proposed approach. Each data set contains a high-resolution PAN image and a low spatial resolution MS image composed of four different bands (blue, green, red, and near infrared). The first data set, as shown in Fig. 2(a) and (b), was collected by the ZiYuan-3 (ZY-3) satellite on the area of Wuhan, China, which provides the PAN band at 2.1-m resolution and the MS bands at 5.8-m resolution. The second data set, as shown in Fig. 2(e) and (f), was collected by the GeoEye-1 satellite on the area of Hobart, Australia, which provides the PAN band at 0.5-m resolution and the MS bands at 2-m resolution. Due to the insignificant variations of the terrain height in the small areas of the two data sets, the influence of the terrain elevation across the whole image is ignored in our experiments.

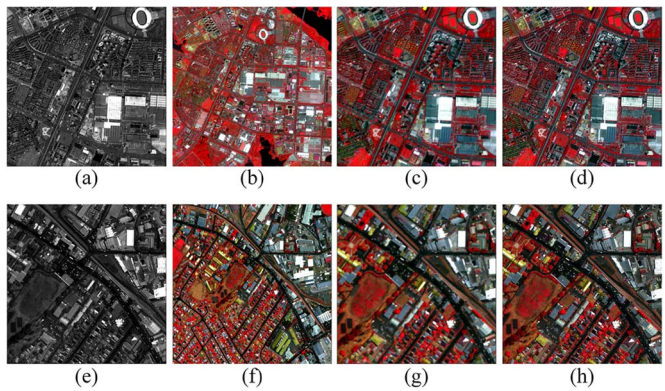

Fig. 2. Source images, registered images, and fused results of proposed approach for two data sets (displayed in a color-infrared manner). (a) ZY-3 PAN image, 1024 × 1024 pixels. (b) ZY-3 MS image, 745 × 747 pixels. (c) Registered image of JPSF for ZY-3 data set. (d) Fused image of JPSF for ZY-3 data set. (e) GeoEye-1 PAN image, 1024 × 1024 pixels. (f) GeoEye-1 MS image, 503 × 460 pixels. (g) Registered image of JPSF for GeoEye-1 data set. (h) Fused image of JPSF for GeoEye-1 data set.

B. Compared Methods

To evaluate the effectiveness of the proposed approach, the proposed joint processes of registration and fusion are compared with the separate processes of registration and fusion. In these experiments, the SVR method [17] is chosen to produce the fused image. The following registration methods are implemented and used for comparison.

1) SIFT registration method. SIFT matched features are first obtained from PAN and MS images using nearest neighborhood distance ratio [18] and random sample consensus (RANSAC) [19], where the threshold of the distance ratio is 0.8. Then, the affine transformation parameters are estimated by least square solution.
2) The registration method combines SIFT features and normalized cross-correlation (NCC) control points (CPs) (SIFT+NCC) [20]. The details of extracting SIFT and NCC CPs, which are used to estimate the affine transformation parameters, are described in [20].

In these experiments, the principal component analysis is used to convert the MS image from multiband to single band in order to extract SIFT features from the MS image effectively [4].

C. Experimental Results

In this section, we evaluate the registration accuracy and fusion performance of the proposed joint approach, respectively. To demonstrate the advantage of the proposed approach, joint processes of SIFT and SVR (JPSF) and joint processes of SIFT+NCC and SVR (JPSN) are compared with a separate scheme with SIFT and SVR (SSF) and a separate scheme with SIFT+NCC and SVR (SSN). In these experiments, we set $N_{it} = 100$, $\varepsilon = 10^{-5}$, $\lambda = 0.1$, and $\{n_i, i = 1, 2, \ldots, 6\} = \{1, 10^{-2}, 10^{-2}, 1, 10^{-2}, 10^{-2}\}$.

TABLE I
QUANTITATIVE RESULTS OF SSF, JPSF, SSN, AND JPSN METHODS IN ZY-3 AND GEOEYE-1 DATA SETS. CC, ERGAS, AND Q4 ARE USED TO EVALUATE THE FUSION QUALITY. RMSE AND RMS_{LOO} ARE USED TO EVALUATE THE REGISTRATION ACCURACY. *: UNIT IS PIXEL

		ZY-3				GeoEye-1			
		SSF	JPSF	SSN	JPSN	SSF	JPSF	SSN	JPSN
CC	B	0.911	0.952	0.942	**0.953**	0.876	**0.936**	0.922	**0.936**
	G	0.911	0.953	0.943	**0.954**	0.876	**0.936**	0.923	**0.936**
	R	0.910	0.952	0.942	**0.953**	0.877	0.938	0.925	**0.939**
	NIR	0.922	**0.959**	0.947	0.958	0.892	**0.945**	0.932	**0.945**
Q4		0.903	**0.949**	0.938	**0.949**	0.873	**0.937**	0.923	**0.937**
ERGAS		2.244	1.637	1.651	**1.633**	5.121	3.674	3.769	**3.660**
RMSE*		1.936	0.793	1.069	0.735	1.964	0.951	1.120	0.903
RMS^*_{LOO}		2.171	0.232	0.868	0.211	1.718	0.196	0.835	0.155

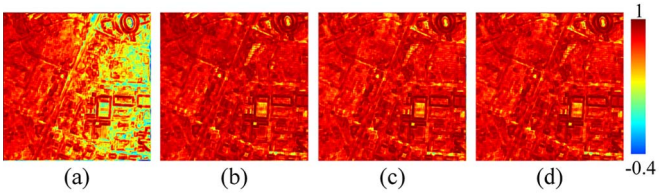

Fig. 3. Color-coded image of ZY-3 normalized correlation coefficients. (a) NCC result of SSF. (b) NCC result of JPSF. (c) NCC result of SSN. (d) NCC result of JPSN.

1) Registration Accuracy Evaluation: Fig. 2(c) and (d) shows the registered and fused results of JPSF for the ZY-3 data set, while Fig. 2(g) and (h) shows the registered and fused results of JPSF for the GeoEye-1 data set.

To evaluate the accuracy of the registration process, we applied two different methods. One is based on the RMSE and RMS_{LOO} [21]. Ten manually selected CPs, which were uniformly distributed in the PAN and original MS images, were used to calculate the RMSE according to (7) shown at the bottom of the page, where (x_i, y_i) and (u_i, v_i) denote the coordinates of the ith manual CPs. For the SSF and SSN methods, matched feature points are used to compute the RMS_{LOO}. For the JPSF and JPSN methods, we first divided the PAN image into tiles of size 128 × 128 pixels, and then, we obtained a set of tie points based on the center of the tiles by the iterative optimization algorithm. Table I shows the RMSE and RMS_{LOO} results of all the methods. The other method is taken from [22]. Once the MS image had been registered, we first generated the low spatial resolution synthetic PAN image, whose detailed explanation can be found in [17], and then, we computed the NCC over local windows (21 by 21) for each pixel between the PAN image and the synthetic PAN image. Due to the space limitation, only the NCC results of the ZY-3 data set are shown in Fig. 3.

From Table I, it is clearly demonstrated that the image registration, using the proposed joint approach, results in lower RMSE and RMS_{LOO} and can achieve the subpixel accuracy.

By visual inspection of the NCC results, it would not be difficult to find that the NCC results of JPSF, SSN, and JPSN are higher than that of SSF across the whole image, particularly

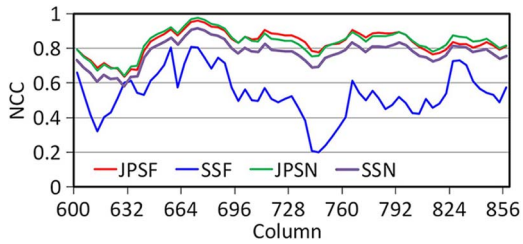

Fig. 4. Partial NCC analysis of SSF, JPSF, SSN, and JPSN methods in ZY-3 data set.

on the right portion of the image. To investigate the quantitative analysis of the NCC results, a group of pixels extracted at line 512 from the NCC results is chosen and compared in this test. Fig. 4 shows the partial comparisons of NCC pixels from column 600 to column 856. It can be noted that the NCC of the proposed joint processes (JPSF and JPSN) are higher than the NCC of the separate processes (SSF and SSN). Most of the NCC pixels of JPSF and JPSN are above 0.8, while the majority of the NCC pixels of SSF are about 0.6 or even lower. In general, both methods and comparative results indicate that the proposed joint approach achieves higher performance in registration.

2) Comparisons on Fusion Performance: In order to evaluate the fusion performance of the proposed approach, the CC, Q4 (averages on 32 × 32 blocks), and ERGAS indexes are measured between the fused and the registered MS images. ERGAS should be as low as possible, whereas CC and Q4 should approach to 1. Table I lists the quantitative scores of all methods. From Table I, one can see that the proposed joint approach outperforms the separate scheme with registration and fusion methods in terms of these indexes. The comparison results further confirmed the advancement of the proposed joint approach in registration accuracy.

D. Comparison With Other Objective Functions

In this section, we discuss the influence of different objective functions on our approach. In these experiment, CC, mutual information (MI), and ERGAS index are chosen to construct the objective functions. The SIFT method and SVR method are selected for the registration and fusion processes. The fusion steps are ignored in the iterative optimization process for the CC and MI objective functions because their values are computed between the PAN and the registered MS images. Additionally, the greater the CC and MI values are, the higher the registration accuracy is. Hence, the CC and MI are inverted to satisfy (2). Table II shows the results of the registration accuracy and the fusion quality with the different objective functions. From the experimental results, we can draw the following conclusions. The proposed approach using the fusion quality, i.e., ERGAS, as a measure of the registration accuracy achieves higher registration and fusion performance in terms of RMS^*_{LOO}, Q4, and ERGAS index.

$$\mathrm{RMSE} = \sqrt{\frac{1}{10}\sum_{i=1}^{10}\left(x_i - (p_1 + p_2u_i + p_3v_i)\right)^2 + \left(y_i - (p_4 + p_5u_i + p_6v_i)\right)^2} \tag{7}$$

TABLE II
COMPARISONS ON THE PROPOSED APPROACH WITH DIFFERENT OBJECTIVE FUNCTIONS USING RMS^*_{LOO}, Q4, AND ERGAS MEASURES IN ALL DATA SETS. OBJECTIVE FUNCTIONS F_{CC}, F_{MI}, AND F_{ERGAS} ARE CONSTRUCTED BY CC, MI, AND ERGAS INDEX, RESPECTIVELY. *: UNIT IS PIXEL

	ZY-3			GeoEye-1		
	RMS^*_{LOO}	Q4	ERGAS	RMS^*_{LOO}	Q4	ERGAS
F_{CC}	0.354	0.941	1.648	0.321	0.929	3.751
F_{MI}	0.252	0.947	1.642	0.318	0.930	3.740
F_{ERGAS}	0.232	0.949	1.637	0.196	0.937	3.674

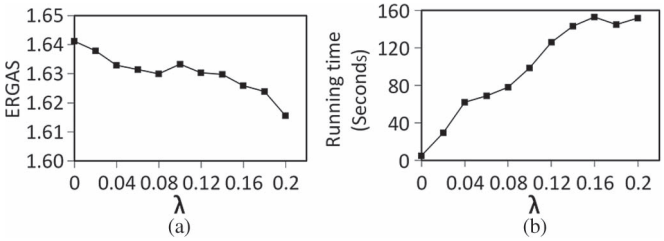

Fig. 5. Computation cost and ERGAS of the JPSN with different λ values in ZY-3 data set.

TABLE III
COMPUTATION COST OF SSF, JPSF, SSN, AND JPSN METHODS IN ZY-3 AND GEOEYE-1 DATA SETS. $^{\alpha}$ METHOD NEEDS NO ITERATION

	ZY-3				GeoEye-1			
	SSF	JPSF	SSN	JPSN	SSF	JPSF	SSN	JPSN
Iterations	$^{\alpha}$	13	$^{\alpha}$	9	$^{\alpha}$	19	$^{\alpha}$	14
Running time(Seconds)	12.902	133.194	17.888	99.092	13.215	228.107	20.327	152.643

E. On the Parameter λ in the Iterative Optimization Procedure

In this section, we analyze the effects of the parameter λ in our approach. In these experiments, we choose the ZY-3 data set and the JPSN method. Fig. 5(a) shows the ERGAS index with respect to the variation of λ. Fig. 5(b) provides the running time with respect to the variation of λ. Experimental results demonstrate that the ERGAS will decrease with the increase of λ, whereas the computation cost increases.

F. Computation Cost Analysis

In this section, we discuss the computation cost of the proposed approach. All the experiments are conducted on a PC with Intel i3-3220 3.3 GHz and 4-GB memory. Each experiment is repeated five times, and the average running time of the proposed approach applied on two data sets is presented in Table III. As shown in the table, although the proposed approach consumes a lot of time, the JPSN method has performed much better than the JPSF method. It is because the iterative optimization process is a time-consuming task and the time consumption will increase due to the low precision of the initial affine transformation parameters.

IV. CONCLUSION

In this letter, a novel joint image registration and fusion approach for PAN and MS images has been presented. This approach adopts the fusion performance to evaluate the registration accuracy and constructs an objective function to update the registration parameters iteratively. Experiments and comparisons have shown that the results obtained with the proposed approach have higher registration accuracy and fusion quality, although the iterations will increase the time consumption. Regarding the registration of large scenes with the significant difference in terrain elevation, the affine transformation model applied in our work is not suitable. In our future work, we will make improvements to the efficiency and the robustness of the proposed approach, particularly for the large-size images with widely varied terrain height, and we will make the joint optimization framework applicable for image registration and change detection.

ACKNOWLEDGMENT

The authors would like to thank Dr. Q. Zou (Wuhan University) for his valuable comments and advices and the anonymous reviewers for their highly constructive and outstanding remarks.

REFERENCES

[1] B. Zitova and J. Flusser, "Image registration methods: A survey," *Image Vis. Comput.*, vol. 21, no. 11, pp. 977–1000, Oct. 2003.
[2] Y. Bentoutou, T. Nasreddine, K. Kidiyo, and R. Joseph, "An automatic image registration for applications in remote sensing," *IEEE Trans. Geosci. Remote Sens.*, vol. 43, no. 9, pp. 2127–2137, Sep. 2005.
[3] D. G. Lowe, "Distinctive image features from scale-invariant keypoints," *Int. J. Comput. Vis.*, vol. 60, no. 2, pp. 91–110, Nov. 2004.
[4] H. Goncalves, L. Cortereal, and J. A. Goncalves, "Automatic image registration through image segmentation and SIFT," *IEEE Trans. Geosci. Remote Sens.*, vol. 49, no. 7, pp. 2589–2600, Jul. 2011.
[5] Y. Zhang, "Understanding image fusion," *Photogramm. Eng. Remote Sens.*, vol. 70, no. 6, pp. 657–661, Jun. 2004.
[6] B. Aiazzi, S. Baronti, F. Lotti, and M. Selva, "A comparison between global and context-adaptive pansharpening of multispectral images," *IEEE Geosci. Remote Sens. Lett.*, vol. 6, no. 2, pp. 302–306, Apr. 2009.
[7] C. K. Munechika, J. S. Warnick, C. Salvaggio, and J. R. Schotto, "Resolution enhancement of multispectral image data to improve classification accuracy," *Photogramm. Eng. Remote Sens.*, vol. 59, no. 1, pp. 67–72, Jan. 1993.
[8] H. Wang, W. Jiang, C. Lei, S. Qin, and J. Wang, "A robust image fusion method based on local spectral and spatial correlation," *IEEE Geosci. Remote Sens. Lett.*, vol. 11, no. 2, pp. 454–458, Feb. 2014.
[9] L. Wald, "Quality of high resolution synthesized images: Is there a simple criterion?" in *Proc. Int. Conf. Fusion Earth Data*, 2000, pp. 99–105.
[10] Z. Wang and A. C. Bovik, "A universal image quality index," *IEEE Signal Process. Lett.*, vol. 9, no. 3, pp. 81–84, Mar. 2002.
[11] V. S. Petrovic and C. S. Xydeas, "Gradient-based multiresolution image fusion," *IEEE Trans. Image Process.*, vol. 13, no. 2, pp. 228–237, Feb. 2004.
[12] Z. Li, S. Chen, H. Leung, and E. Bosse, "Joint data association, registration, fusion using EM-KF," *IEEE Trans. Aerosp. Electron. Syst.*, vol. 46, no. 2, pp. 496–507, Apr. 2010.
[13] S. Chen, Q. Guo, H. Leung, and E. Bosse, "A maximum likelihood approach to joint image registration and fusion," *IEEE Trans. Image Process.*, vol. 20, no. 5, pp. 1363–1372, May 2011.
[14] Y. S. Kim, J. H. Lee, and J. B. Ra, "Multi-sensor image registration based on intensity and edge orientation information," *Pattern Recognit.*, vol. 41, no. 11, pp. 3356–3365, Nov. 2008.
[15] J. A. Nelder and R. Mead, "A simplex method for function minimization," *Comput. J.*, vol. 7, no. 4, pp. 308–313, Jan. 1965.
[16] W. H. Press, S. A. Teukolsky, W. T. Vetterling, and B. P. Flannery, *Numerical Recipes in C++—The Art of Scientific Computing*. Cambridge, U.K.: Cambridge Univ. Press, 2002, pp. 413–417.
[17] Y. Zhang, "A new merging method and its spectral and spatial effects," *Int. J. Remote Sens.*, vol. 20, no. 10, pp. 2003–2014, Jan. 1999.
[18] K. Mikolajczyk and C. Schmid, "A performance evaluation of local descriptors," *IEEE Trans. Pattern Anal. Mach. Intell.*, vol. 27, no. 10, pp. 1615–1630, Oct. 2005.
[19] M. Fischler and R. Bolles, "Random sample consensus: A paradigm for model fitting with applications to image analysis and automated cartography," *Commun. ACM*, vol. 24, no. 6, pp. 381–395, Jun. 1981.
[20] J. Ma, J. C. Chan, and F. Canters, "Fully automatic subpixel image registration of multiangle CHRIS/Proba data," *IEEE Trans. Geosci. Remote Sens.*, vol. 48, no. 7, pp. 2829–2839, Jul. 2010.
[21] H. Goncalves, J. A. Goncalves, and L. Cortereal, "Measures for an objective evaluation of the geometric correction process quality," *IEEE Geosci. Remote Sens. Lett.*, vol. 6, no. 2, pp. 292–296, Apr. 2009.
[22] S. Leprince, S. Barbot, F. Ayoub, and J. P. Avouac, "Automatic and precise orthorectification, coregistration, subpixel correlation of satellite images, application to ground deformation measurements," *IEEE Trans. Geosci. Remote Sens.*, vol. 45, no. 6, pp. 1529–1558, Jun. 2007.